

**Effect of  $\text{TiO}_2$  Addition in  $\text{Al}_2\text{O}_3$ :  
Phase Evolution, Densification, Microstructure And  
Mechanical Properties**

**A**

**THESIS SUBMITTED IN THE PARTIAL FULFILLMENT OF  
THE REQUIREMENT FOR THE DEGREE OF  
BATCHLOR OF TECHNOLOGY**

**IN**

**CERAMIC ENGINEERING**

**BY**

**SNEHLATA KUMARI**

**Roll No-109CR0676**



**DEPARTMENT OF CERAMIC ENGINEERING  
NATIONAL INSTITUTE OF TECHNOLOGY, ROURKELA**

**2013**

**Effect of  $\text{TiO}_2$  Addition in  $\text{Al}_2\text{O}_3$ :  
Phase Evolution, Densification, Microstructure And  
Mechanical Properties**

**A**

**THESIS SUBMITTED IN THE PARTIAL FULFILLMENT OF  
THE REQUIREMENT FOR THE DEGREE OF  
BATCHLOR OF TECHNOLOGY**

**IN**

**CERAMIC ENGINEERING**

**BY**

**SNEHLATA KUMARI**

**Roll No-109CR0676**

**Under the guidance of  
Prof. Ranabrata Mazumder**



**DEPARTMENT OF CERAMIC ENGINEERING  
NATIONAL INSTITUTE OF TECHNOLOGY, ROURKELA**

**2013**

## Acknowledgement

I would like to express my heart felt gratitude to **Prof. R. Mazumder**, Dept. of Ceramic Engineering, NIT Rourkela for suggesting the topic for my thesis and for their ready and able guidance throughout the course of my preparing the report. Under his guidance, the final year project can be completed in accordance of the planned schedule. I thank you Sir for your help, inspiration and blessings.

I express my sincere thanks to **Prof. S. K. Pratihari**, Head of the Department of Ceramic Engineering, NIT Rourkela for providing me the necessary facilities in the department. I would express my gratitude and sincere thanks to my honorable teachers **Prof. Santanu Bhattacharyya, Prof. J. Bera, Dr. B. B. Nayak, Dr. S. K. Pal and Mr. A. Chowdhury** for their invaluable advice, constant help, encouragement, inspiration and blessings. My very special thanks to **Prof. R. Mazumder** for his constant help throughout the project work.

Submitting this thesis would have been a Herculean job, without the constant help, encouragement, support and suggestions from my seniors and friends, especially Ganesh sir, Patibha Didi, Gita didi, for their time to help. Although it will be difficult to record my appreciation to each and every one of them in this small space; I will relish your memories for years to come.

Last but not the least I would like to thank my parents and family members for their support, blessing and affection. I would also express my sincere thanks to staff members of Ceramic Engineering Department, N.I.T. Rourkela.

Date:

SNEHLATA KUMARI

109CR0676

## CERTIFICATE

This is to certify that the thesis on “**Effect of TiO<sub>2</sub> Addition in Al<sub>2</sub>O<sub>3</sub>: Phase Evolution, Densification, Microstructure And Mechanical Properties**” submitted by **Miss Snehlata kumari**, to the National Institute of Technology, Rourkela in partial fulfillment of the requirements for the award of the degree of **Bachelor of Technology in Ceramic Engineering** is a record of bonafide research work carried out by her under my supervision and guidance. Her thesis, in our opinion, is worthy of consideration for the award of degree of Bachelor of Technology in accordance with the regulations of the institute.

The results embodied in this thesis have not been submitted to any other university or institute for the award of a Degree.

Supervisor

Prof. R. Mazumder  
Department of Ceramic Engineering  
National Institute of Technology  
Rourkela

## Abstract

The thesis describes the effect of  $\text{TiO}_2$  addition in alumina on phase formation, densification, microstructure and mechanical properties of the composite. The ceramic composite were prepared with  $\text{Al}_2\text{O}_3$  and  $\text{TiO}_2$  powder by solid state mixing route. The  $\text{Al}_2\text{O}_3$ - $\text{TiO}_2$  powders contain 3, 5, 10, 13, 20, and 40 wt% of  $\text{TiO}_2$ . Mixed powders were calcined at  $1200^\circ\text{C}$ . Calcined powders were uniaxially pressed into cylindrical pellets and rectangular bars, and sintered at  $1600^\circ\text{C}$ . X-ray powder diffraction technique was used to study the phase evolution in calcined powder and in sintered specimen. Scanning electron microscope (SEM) was used to find out the particle size and powder morphology of calcined powder and microstructure of sintered sample. Flexural strength and Vickers hardness were measured on sintered sample.

Calcined powder contains only alumina and titania phase. No intermediate phase was detected. In sintered sample  $\text{Al}_2\text{TiO}_5$  phase was detected and its concentration increases with increases in  $\text{TiO}_2$  content.  $\text{TiO}_2$  phase was disappeared for high amount of  $\text{TiO}_2$  (20 and 40wt% addition). It was found that low concentration of  $\text{TiO}_2$  (upto 10wt %) increases the density of the composite and further increase in  $\text{TiO}_2$  concentration density decreases rapidly. Presence of  $\text{Al}_2\text{TiO}_5$  phase restricts the grain growth of alumina phase. Flexural strength and Vickers hardness of  $\text{Al}_2\text{O}_3$ - $\text{TiO}_2$ - $\text{Al}_2\text{TiO}_5$  composite is dependent on the content of  $\text{TiO}_2$  and the presence of  $\text{Al}_2\text{TiO}_5$  phase.

## **List of figures:**

**Figure 1:** Structure of alumina, containing aluminium atoms and oxygen atoms

**Figure 2:** Unit cell of rutile  $\text{TiO}_2$

**Figure 3** Phase diagram of  $\text{Al}_2\text{O}_3$ - $\text{TiO}_2$  system

**Figure 4:** Flow chart for work plan

**Figure 5:** Vickers hardness tester and diamond like indentation

**Figure 6:** Schematic of three - point bending flexural strength test

**Figure 7:** XRD plot of powder of different composition, calcined at  $1200^\circ\text{C}$

**Figure 8:** SEM micrograph of 3% and 13%  $\text{TiO}_2$  -doped alumina sintered at  $1600^\circ\text{C}$  for 2hrs

**Figure 9:** XRD pattern for sintered samples.

**Figure 10:** Plot for variation of relative density and bulk density with  $\text{TiO}_2$  content.

**Figure11:** SEM micrograph of AT-3 and AT-13 sample sintered at  $1600^\circ\text{C}$  for 2hrs

**Figure 12:** SEM micrograph of AT-20 and AT-40 sample sintered at  $1600^\circ\text{C}$  for 2hrs.

**Figure 13:** Flexural strength of different  $\text{TiO}_2$  added sample sintered at  $1600^\circ\text{C}$

**Figure 14:** Vickers hardness of different  $\text{TiO}_2$  added sample sintered at  $1600^\circ\text{C}$

## List of tables

**Table 1:** Mechanical Properties of Aluminium Oxide (99 - 99.9 wt %)

**Table 2:** values for bulk density, relative density and percent of phase present of different compositions sintered at 1600°C.

**Table3:** Flexural strength in MPa for different percentage of TiO<sub>2</sub> in alumina.

**Table 4:** Values of hardness (GPA) for different compositionof alumina and TiO<sub>2</sub>

# CONTENTS

*Abstract*

*List of Figures*

*List of tables*

<b>Chapter 1</b> INTRODUCTION	2-3
<b>Chapter 2</b> LITERATURE REVIEW	5-11
2.1 Alumina	
2.2 Titania	
2.3 Aluminium-titanate( $\text{Al}_2\text{TiO}_5$ )	
2.4 Effect of $\text{TiO}_2$ addition on solid solubility, densification and mechanical properties	
<b>Chapter 3</b> MOTIVATION, OBJECTIVE AND WORK PLAN	13-14
<b>Chapter 4</b> EXPERIMENTAL WORK	16-19
4.1 Powder synthesis and Characterization	
4.2 Powder compaction and sintering	
4.3 Sintered pellets characterization	
4.4 Phase analysis-X ray diffraction	
4.5 Microstructure analysis-SEM	
4.6 Mechanical properties measurement	
<b>Chapter 5</b> RESULTS AND DISCUSSION	21-32
5.1 Phase Analysis of calcined powder	
5.2 Morphology of calcined powders	
5.3 Phase Analysis of sintered samples	
5.4 Densification behavior	
5.5 Microstructure of sintered samples	
5.6 Mechanical properties	
5.6.1 Flexural strength	
5.6.2 Vickers Hardness	



**Chapter 6 CONCLUSIONS**

34

**REFERENCES**

35-36

## **Chapter 1**

# **INTRODUCTION**

## Introduction:

Composites of alumina and titania are known for their high toughness, low thermal expansion, and low thermal conductivity. These properties make alumina-titania composites desirable materials of construction and coatings for high performance applications where thermal barriers are required [1, 2].

Alumina-titania coatings are excellent candidates for providing protection against abrasive wear, and are resistant to high temperature erosion with cryogenic compatibility. It has high thermal shock resistance. With addition of titania wear resistance increases, adhesion strength increases but hardness decreases. Thermal expansion coefficient of alumina and titania are 8 and  $7.5(10^{-6} \text{K}^{-1})$ . Due to the Stefan-Boltzmann law (radiated power  $\propto T^4$ ) the 300 K radiation is dominant compared to the radiation from the shielding at 85 K. Therefore, the many parts of the radiation shield must be blackened of the radiation shielding facing to charcoal coated cryopanel in Cryopump. Metals have a low emissivity over the whole spectrum and thus cannot dissipate heat by radiating in the thermal infrared region. It is well known that most polar bonding oxides show strong efficiency of photon emission thus exhibiting a high emissivity value. Wang et.al reported emissivity of modified  $\text{Al}_2\text{O}_3$  coating on aluminum surface [3].

Some publications have pointed out the potential of  $\text{Al}_2\text{O}_3/\text{TiO}_2$  thermally sprayed coatings for diverse applications on components of fusion reactors [4]. However, scarce information is found in the literature about the optimal processing of these coatings regarding their emissive capability and about the influence of the powder and phase composition on the functionality of the coatings. Cockeram et. al. used different oxide based coating for enhancement of thermal emissivity of radiator for thermo photovoltaic (TPV) power generation system. They plasma sprayed two different commercially available  $\text{Al}_2\text{O}_3\text{-TiO}_2$  composition, but not disclosed exact composition. Very high emissivity ( $>0.9$ ) was reported for one composition [5]. The other applications of  $\text{Al}_2\text{O}_3\text{-TiO}_2$  composites are

- $\text{TiO}_2/\text{Al}_2\text{O}_3$  films for optical application.
- $\text{Al}_2\text{O}_3/\text{TiO}_2$  nanocomposites to use in the femoral head of hip replacement
- Hydraulic parts
- Plungers

- Automotive parts
- Textile manufacturing components and tooling
- Components for the chemical industry
- Electrical insulation and dielectric applications - Bioelectronic dielectric materials for sensor packaging and biochips

## **Chapter 2**

# **LITERATURE REVIEW**

## 2.1 Al<sub>2</sub>O<sub>3</sub>

Al<sub>2</sub>O<sub>3</sub> is an oxide of aluminum a group III element. It is known to be a very stable and robust material. It possesses strong ionic interatomic bonding giving rise to its desirable material characteristics. Alumina is well known for its high strength and stiffness. The material's hardness is extremely high resulting in its low wear. It can exist in several crystalline phases. The most stable hexagonal alpha phase is of particular interest for structural applications. The oxygen ions form a hexagonal close-packed structure with aluminium ions filling two-thirds of the octahedral interstices. Each Al<sup>3+</sup> center is octahedral.

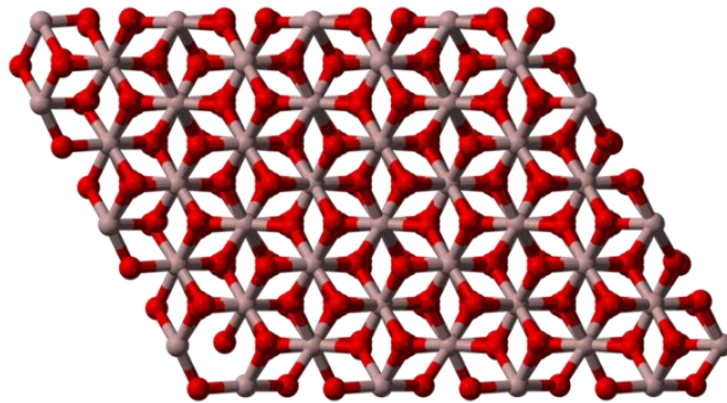


**Figure 1:** structure of alumina containing aluminium atoms and oxygen atoms [6].

Alpha phase alumina is the strongest and stiffest of the oxide ceramics. Alumina is well known for its high hardness. Its high hardness, excellent dielectric properties, refractoriness and good thermal properties make it the material of choice for a wide range of applications. However, due to its intrinsic stiff and brittle characteristics, alumina exhibits design limitations. Flexural strength of alumina, which is a mechanical parameter associated with brittleness, is low, making it unable to resist deformation under load over an extended period of time [7].

In addition, the strength of alumina strongly depends on the types of acting forces or stresses as a result of low fracture toughness and the presence of imperfections. As with other ceramic-based materials, alumina has a higher degree of compressive strength; it is relatively brittle in nature under tensile and bending stresses. Additives can be added to enhance particular desirable material characteristics. An example would be the addition of chrome oxide or manganese oxide to

improve hardness and change color.  $\text{TiO}_2$  addition in alumina increases its fracture toughness. Other additions can be made to improve the different properties of composition [8].

**Table 1:** Mechanical Properties of Aluminium Oxide (99 - 99.9 wt%) [11]

Hardness	15-16 GPa
Flexural Strength	550 MPa
Tensile Strength	310 MPa
Compressive Strength	3790 MPa
Fracture Toughness	4.0 MPa.m
Modulus of Elasticity	330-400 GPa

### Other properties of $\text{Al}_2\text{O}_3$

- Excellent dielectric properties
- Good thermal conductivity
- Excellent size and shape capability
- It is available in different purity ranges from 94%, an easily metallizable composition, to 99.8% for the most demanding high temperature applications.
- Resists strong acid and alkali attack at elevated temperatures

High purity alumina is usable in both oxidizing and reducing atmospheres to  $1925^\circ\text{C}$ . It resists attack by all gases except wet fluorine and is resistant to all common reagents except hydrofluoric acid and phosphoric acid. Elevated temperature attack occurs in the presence of alkali metal vapors particularly at lower purity levels.

## 2.2 TiO<sub>2</sub>

Three different crystallographic structures of TiO<sub>2</sub> (titania) occur in nature: Rutile -tetragonal, Anatase-tetragonal, Brookite –orthorhombic. Out of these three polymorphs of TiO<sub>2</sub>, only rutile is the thermodynamically most stable phase where as anatase and brookite is metastable, transforming to rutile when they are heated. Brookite transforms into rutile at quite low temperatures. Only the rutile and anatase play a significant role in industrial applications. Applications of brookite are limited due to its rareness and difficult preparation [9, 10].

Figure 2 shows a schematic of a unit cell of rutile TiO<sub>2</sub>. However, anatase is typically the majority product of inorganic syntheses and is the main constituent of nanocrystalline materials. It has been reported that titania normally undergoes anatase - rutile phase transformation in the temperature range from 600 to 700°C.

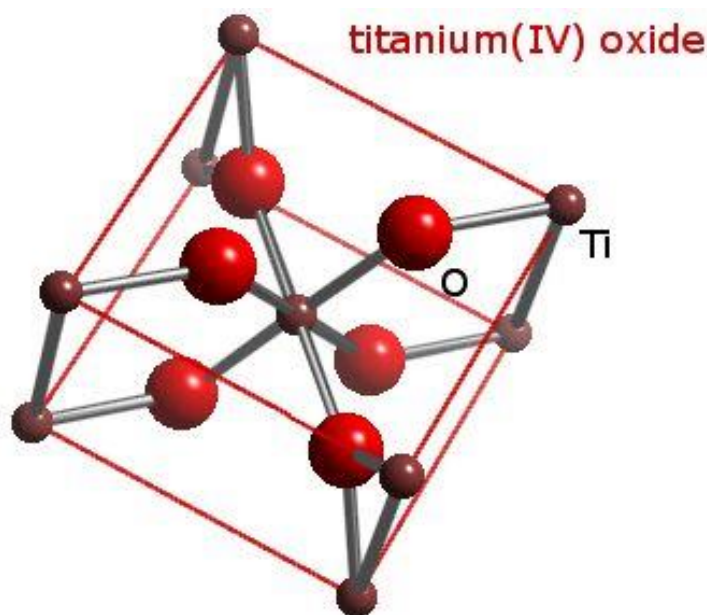


Figure 2. Unit cell of rutile TiO<sub>2</sub> [11].

Titanium oxide (TiO<sub>2</sub>)-based ceramics have many desirable and potential applications. Their mechanical properties are strongly affected by composition and microstructure, and can thus be tailored. The optical properties of TiO<sub>2</sub> are useful, being colorless, transparent, and possessing a high refractive index. These properties and the ability to



tailor the structure make  $\text{TiO}_2$ -based ceramics suitable for a wide range of applications. [10]

- As a semiconductor material with long-term stability, non-toxic environmental acceptability and broadly low cost availability  $\text{TiO}_2$  has also been taken into account for photovoltaic applications [17].
- Wide transmission range strong birefringency and good mechanical properties of rutile make it suitable for fabrication of polarizing cubes, prisms and optical isolators.

### 2.3 Aluminum- titanate ( $\text{Al}_2\text{TiO}_5$ )

$\text{Al}_2\text{TiO}_5$  is a synthetic ceramic material, it is considered as a candidate for many structural applications because of its high melting point, low thermal conductivity, almost zero thermal expansion and excellent thermal shock resistance [11]. Thus it is being tested as an insulator material in combustion engines, e.g. as port liner in the cylinder head, piston head, manifold, lining of turbochargers, swirl chamber and valve insulation [12]. It belongs to a class of ceramics having a zero thermal expansion coefficient and excellent thermal shock resistance. It develops microcracks in the cooling step after sintering process. These fine intergranular cracks limit the strength of the material, but provide an effective mechanism for absorbing strain energy during thermal shock and preventing catastrophic crack propagation [11].

Furthermore, it is a good substitute of machinable BN-ceramics which is used as an insulating substrate in current micro-electronic industry and it is very expensive, therefore the development of new low-cost machinable substrate ceramic are consistently required. The results of many researches showed that this composite could be used for low-cost machinable ceramics for the replacement of BN ceramics [12, 13]. It has almost zero thermal expansion coefficient ( $0.8 \times 10^{-8} \text{ }^\circ\text{C}^{-1}$ ) in the range of 20 to  $1000^\circ\text{C}$ . But this material is nevertheless unstable below  $1280^\circ\text{C}$  and it decomposes giving rise to  $\text{Al}_2\text{O}_3$   $\alpha$  and titanium oxide (rutile) by an eutectoid reaction [14].

### Phase diagram of $\text{Al}_2\text{O}_3$ and $\text{TiO}_2$

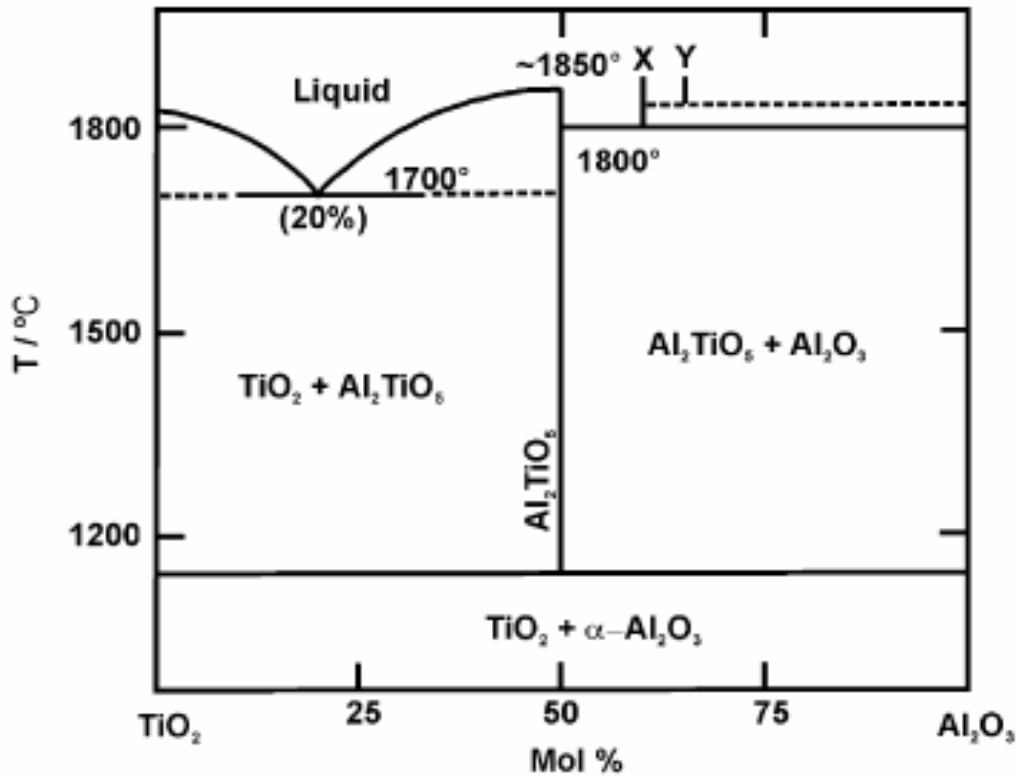


**Figure 3:** Phase diagram of  $\text{Al}_2\text{O}_3$ - $\text{TiO}_2$  system [15]

#### 2.4 Effect of $\text{TiO}_2$ addition on solid solubility, densification and mechanical properties

It is reported [20] that the solid solubility of  $\text{TiO}_2$  in  $\text{Al}_2\text{O}_3$  is too small. It is determined by the lattice parameter shift of  $\text{Al}_2\text{O}_3$ . The solid solution of  $\text{TiO}_2$  in  $\alpha\text{-Al}_2\text{O}_3$  was found at  $>1150^\circ\text{C}$ , and the solubility was 0.27% at  $1300\text{--}1700^\circ\text{C}$ . Beyond the solubility limit, excess  $\text{TiO}_2$  coexisted with  $\alpha\text{-Al}_2\text{O}_3$  as rutile below  $1350^\circ\text{C}$  and as  $\text{Al}_2\text{TiO}_5$  above  $1450^\circ\text{C}$ . The addition of  $\text{TiO}_2$  also promoted the grain growth of  $\text{Al}_2\text{O}_3$ . It was seen that there is decrease in grain size beyond the solubility limit with increasing  $\text{Al}_2\text{TiO}_5$ . That is  $\text{Al}_2\text{TiO}_5$  existing as a second phase retards the grain growth of  $\text{Al}_2\text{O}_3$ .

Wan et al. [1] reported preparation of nanocomposites of alumina and titania by high-energy ball milling. High density composites of alumina and titania with nanosized grains were prepared from aluminium-titanate without using nano size powder as a starting material. The preparation was achieved by high-energy ball milling of the aluminum titanate followed by sintering at elevated temperature and pressure. They prepared aluminium-titanate from micron-sized alumina and titania particles through plasma jet processing.

Hori et al. [2] reported tough corundum-rutile composite sintered body. The sintered body of corundum-alumina and rutile-titania was prepared by adding an alkali metal to an alumina-titania composite powder produced by a vapour-phase reaction of  $\text{AlCl}_3$  and  $\text{TiCl}_4$ . It was claimed that composite body can be sintered to high density within  $1280^\circ\text{C}$ . The sintered body of the invention comprised alumina of corundum phase and titania of rutile phase, which contains alkali metal in an amount of 0.01 to 0.5 wt. % and plate shaped corundum particles whose cross sections having aspect ratios of 2.5 or more are observed to be 10 % or more by scanning electron micrography. This sintered body can have a high toughness by the compounding inexpensive oxides such as alumina and titania. The toughening mechanism of the sintered body was due to a crack deflection effect by geometrically anisotropic particles which are dispersed in the material, and therefore the toughness is not expected to be deteriorated at high temperatures.

Lee et al. [8] prepared alumina-titania bulk composite from high-purity  $\alpha\text{-Al}_2\text{O}_3$  and  $\text{TiO}_2$  powder by hot pressing technique. The wet milling of starting powders was made in a polyethylene jar with alumina balls and 300 ml of ethanol for 24 h. The  $\text{Al}_2\text{O}_3\text{-TiO}_2$  powders contain 0, 5, 10, 15, 20, and 25 mol% of  $\text{TiO}_2$ . The powder mixtures were compacted in a graphite sleeve coated with Boron nitrate (BN), and hot pressing was carried at  $1500^\circ\text{C}$  and 25 MPa, in an Ar gas atmosphere for 1 h. Relative density reduced from 99% to 95% for 5% to 25 mol%  $\text{TiO}_2$  addition. Phase composition in the sintered sample was not reported. High toughness ( $7 \text{ MPa}\cdot\text{m}^{1/2}$ ) is observed at 20 mol%  $\text{TiO}_2$  and high hardness (13 GPa) achieved at composition 10 mol%  $\text{TiO}_2$ . Changes in relative density could be due to formation of  $\text{Al}_2\text{TiO}_5$  because aluminum-titanate has a slightly lower density than alumina and titania. These increments are due to the presence of rutile and aluminum-titanate phases disperse in alumina matrix.

$\text{Al}_2\text{O}_3\text{-TiO}_2$  composite coating was generally prepared by atmospheric plasma spraying. Properties of coating done by 13% titania shows better results than 3% titania, and 40% titania powder. The increase in titania content increases the coating fracture toughness but hardness

decreases. It also says alumina powders are also the most suitable candidates for biomedical applications and electrical. But coating done by these compositions do not have as high a fracture toughness as alumina 13% titania. It has been seen that alumina 3% titania coatings having a higher fracture toughness compared to pure alumina, but it is inferior to coatings of alumina 13% titania [11].

Serkan A ball [15] reported mechanical property of higher amount of  $\text{TiO}_2$  in alumina (40 and 48 %  $\text{TiO}_2$ ). According to this The micro hardness values of the  $\text{Al}_2\text{O}_3$ -40 wt%  $\text{TiO}_2$  are slightly higher than that of the  $\text{Al}_2\text{O}_3$ -48wt.%  $\text{TiO}_2$ . It is shown that the micro hardness values are depends on the amount of  $\text{TiO}_2$ . This may be attributed to the variation in microstructural differences, porosity and phase distribution. Although, originally a pure  $\text{Al}_2\text{O}_3$  single crystal micro hardness value is 11GPa. Hwang et al. [16] found that the bending strength decreased when the  $\text{TiO}_2$  contents were near the solubility 0.2 wt. % and above 2wt %, where the largest grain size and  $\text{Al}_2\text{TiO}_5$  were shown, respectively. The size effect and the thermal stress due to the difference of thermal expansion coefficients between  $\text{Al}_2\text{O}_3$  and  $\text{Al}_2\text{TiO}_5$  were considered to the major factors for the reduction of the bending strength.

## **Chapter 3**

# **MOTIVATION, OBJECTIVE AND WORK PLAN**

## Motivation

Alumina-titania composites are preferred materials of construction and coatings for high performance applications where thermal barriers are required due to its high toughness, high thermal emissivity, low thermal expansion, and low thermal conductivity and resistant to high temperature erosion with cryogenic compatibility. There are many reports available on plasma spraying of ceramic coatings of  $\text{Al}_2\text{O}_3\text{-TiO}_2$  and its characterization. But there are very few reports available on the  $\text{Al}_2\text{O}_3\text{-TiO}_2$  composite powder synthesis, pressureless sintering and its characterization.

## Objective

The objective of this research was to develop a dense ceramic-ceramic composite system which have good mechanical properties and that can fit into multiple purposes.

- To prepare  $\text{Al}_2\text{O}_3\text{-TiO}_2$  powders containing different amount of  $\text{TiO}_2$  (3, 5, 10, 13, 20, and 40wt %)
- To study the phase evolution in calcined powder and in sintered specimen
- To study the pressureless sintering of  $\text{Al}_2\text{O}_3/\text{TiO}_2$  composite
- To study the microstructure of the composites.
- To study the effect of  $\text{TiO}_2$  addition on flexural strength and hardness of the sintered specimen.

## Work plan

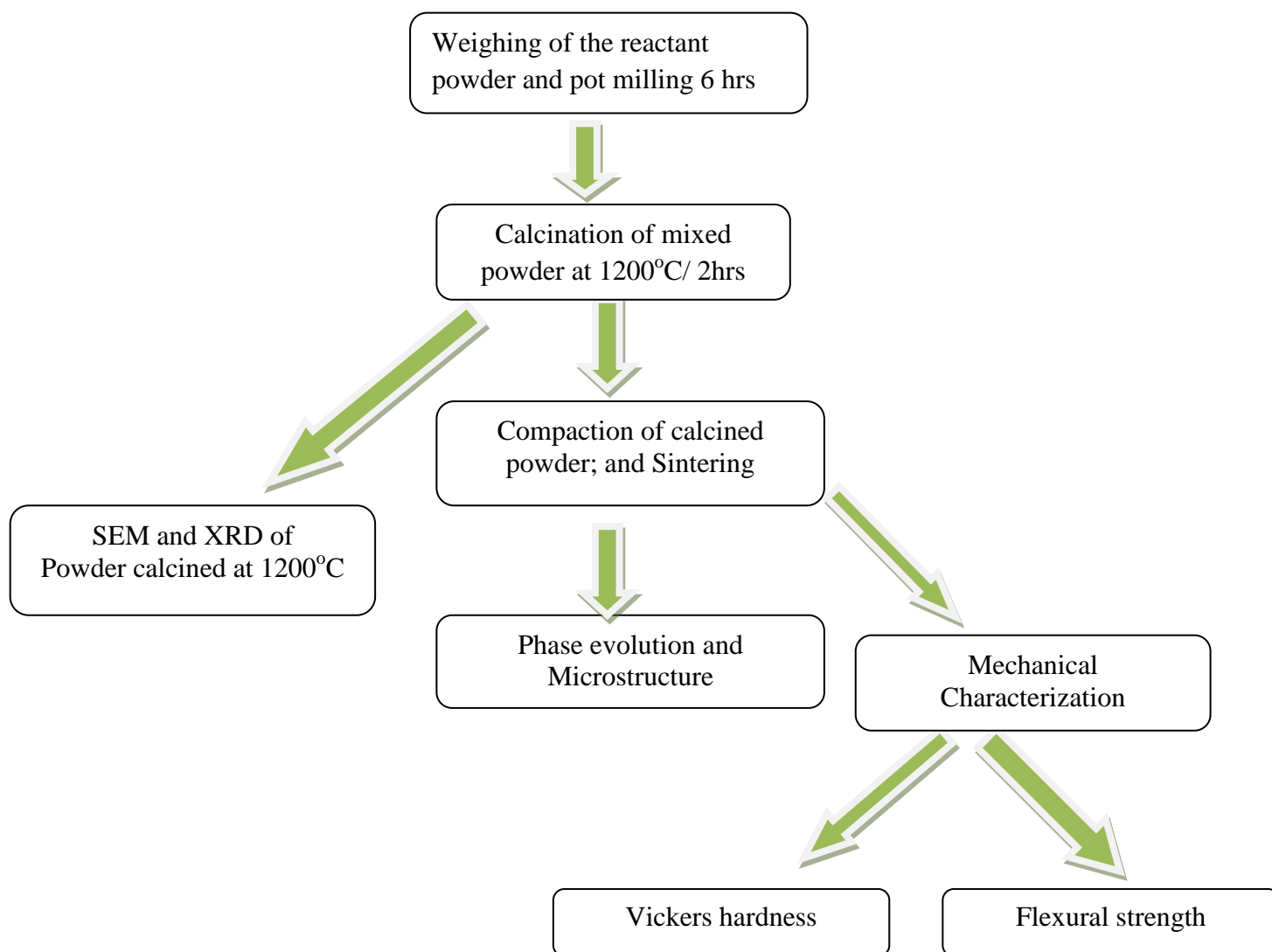


**Figure 4:** Flow chart for work plan

## **Chapter 4**

# **EXPERIMENTAL WORK**



#### **4.1 Powder synthesis and characterization**

Six different composition  $\text{Al}_2\text{O}_3$ - $\text{TiO}_2$  powders was prepared with different percentages of  $\text{TiO}_2$  in  $\text{Al}_2\text{O}_3$  (3, 5, 10, 13, 20, and 40 wt% of  $\text{TiO}_2$ ) and designated as AT-3, AT-5 AT-10 AT-13 AT-20 AT-40, respectively. Powder weighed and then 2-propenal was added to it prepare mixture is the kept for ball milling for 6hrs. Mixed powder is then kept for drying for 1hr and then grinded. The above mixed powder is then kept for calcinations at  $1200^\circ\text{C}$  in furnace. Calcination is a thermal treatment process in which material is heated at a temperature below its melting point to bring a phase transformations decomposition, phase transition, or removal of a volatile fraction. Materials heat treatment to, as in conversion of anatase to rutile phase, anatase to rutile phase transformation takes place at  $900^\circ\text{C}$ . It is also done for decomposition of hydrated minerals.

Structural analysis, phase evolution, phase transformation and morphological characterization of the powder calcined at  $1200^\circ\text{C}$  were carried out using X-Ray Diffraction. Microstructural analysis of the calcined powder was done by using Scanning Electron Microscope.

#### **4.2 Powder compaction and sintering**

Calcined powder is mixed with binder 3% PVA (poly vinyl alcohol) and kept for drying for some time. Binder mixed powder is then compacted uniaxially by using hydraulic press. A stainless steel die with internal die diameter 12.5 mm was used to make pellets. For measurement of modulus of rupture a rectangular shaped bar was compacted of length 50mm. The force used was 4 ton and dwell time was 90 second. Prepared samples then kept in dryer for few hrs. The green compacts were placed on alumina plates and heated from room temperature to  $650^\circ\text{C}$  held for 1 hour at a rate  $5^\circ\text{C}/\text{min}$  for binder removal. Thereafter, the samples were heated to the final sintering temperature  $1600^\circ\text{C}$  with a hold time of 2hrs for desire densification and properties.

The density of Sintered pellets was measure with the help of Archimedes principle. Archimedes' principle a law of physics which states that the upward buoyant force exerted on a body immersed in a fluid equal to the weight of the fluid displaced the body. This principle is true for liquids and gases. Kerosene oil is used as immersion liquid (specific gravity=0.8). First sintered pellets were weighed to take the Dry weight. After taking the weight of the dry pellets it is

poured in kerosene oil in a beaker and then it is kept under vacuum for half an hour to remove the air present in it. Suspended weight was taken in that liquid. Pellets were removed from liquid and then soaked weight was taken. Bulk density was calculated by the following formula.

$$\text{Bulk density} = \frac{\text{dry weight}}{(\text{soaked wt.} - \text{suspended wt.})} \times 0.8$$

$$\text{Relative density} = \frac{\text{bulk density}}{\text{theoretical density}} \times 100$$

#### **4.4 Sintered pellets characterization**

##### **4.4.1 Phase analysis-X ray diffraction**

Pellets were sintered at 1600°C. The phase analysis of that sintered samples was done by X-ray diffraction technique (Philips PAN analytical, The Netherland) using CuK $\alpha$  radiation. The samples were scanned in the 2 $\theta$  ranges 15 to 80°C range in continuous scan mode. The scan rate was 0.02°/sec. Phases present in the sample has been identified with the search match facility available with Philips X'pert high score software. All diffraction methods are based on generation of X-rays in an X-ray tube. The sample, and the diffracted rays are collected These X-rays are directed at. A key component of all diffraction is the angle between the incident and diffracted rays. Powder and single crystal diffraction vary in instrumentation beyond this.

To determine the weight percentage, p, of the compounds detected by XRD, it was assumed that the most intense diffraction peak of each compound was proportional to the percentage in the sample, and it was calculated by Eq.

$$p = \frac{C_i}{\sum_j C} 100$$

Where  $C_i$  represents the integral intensity corresponding to each compound identified, and  $\sum_j C$  is the addition of the integral intensity corresponding to all the compounds identified in the sample

#### 4.4.2 Microstructure analysis-SEM

Microstructure of sintered pellets has been studied using Scanning Electron Microscope (JEOL - JSM 6480LV). The generator voltage was 15 kV. Polished samples were prepared with emery paper of grade P 400 ad P 600 untilla plane and clear surface is attained. Then polished sample is ultrasonicate in acetone to clean theSample.Itwas then thermal etched at a temperature 1500°C below the sintering temperature for half an hour and then it is clean again kept for ultrasonication for 3-4 times. The polished and etched samples were coated with palladium-platinum for 2-3 min. to make the surface conducting. The specimens were observed by SEM in BSE and SE mode.

#### 4.4.3 Mechanical properties measurement

##### Vickers hardness

Sintered pellets are polished and to make surface clear for indentation. The hardness test was studied by a Vickers semi-macro hardness tester (LV-700 Leco, Japan).The indentations were carried out at 3kgf load with 10 sec dwell time. The hardness (Hv) was calculated from the diagonal length using theformula given below

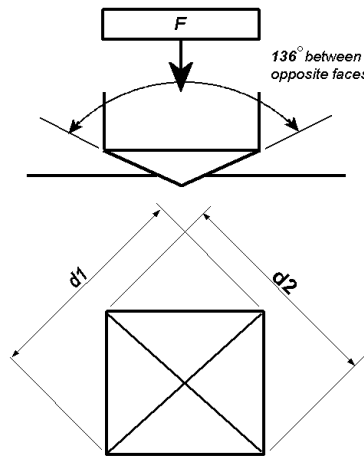


**Figure 5:** Vickers hardness tester and diamond like indentation

$$HV = \frac{2F \sin \frac{136^\circ}{2}}{d^2} \quad HV = 1.854 \frac{F}{d^2} \text{ approximately}$$

Where, F = applied load in Newton

d= half diagonal length in μm.

## Flexural strength

Flexural strength (MOR) is the measure of maximum stress per unit area that a specimen can withstand without breaking when it is bent. In other word it is defined as a material's ability to resist deformation under load. For measuring flexural strength, three-point bending as per ASTM standard C1161-90 was used.

For threepoint bending, the span length was 50 mm. Flexural strength was calculated by using following formula

$$\sigma_{flexural} = \frac{3PL}{2WD^2}$$

Where, P is the fracture load,  $L$  is the span length, W is the width and D is the breadth of the sample

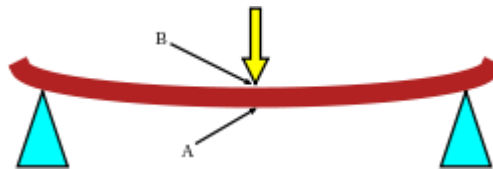


**Figure 6:** schematic of three - point bending flexural strength test

## **Chapter 5**

# **RESULT AND DISCUSSION**

## 5.1 Phase Analysis of calcined powder

The XRD pattern of the calcined powder of different composition was shown in the Fig.7. The XRD pattern shows that the powder crystalline with sharp peaks. These crystalline peaks were identified as  $\text{Al}_2\text{O}_3$  and  $\text{TiO}_2$  only, no  $\text{Al}_2\text{TiO}_5$  phase observed at this stage. Intensity of  $\text{TiO}_2$  phase is increases as the percentage of  $\text{TiO}_2$  in increased in the powder. Temperature used for calcinations was  $1200^\circ\text{C}$  so XRD plot, shows that even for the composition containing higher amount of  $\text{TiO}_2$ , they do not contains any  $\text{Al}_2\text{TiO}_5$  phase that means, at this temperature no reaction is occurring between  $\text{Al}_2\text{O}_3$  and  $\text{TiO}_2$  as alumina and titania starts reaction above  $1300^\circ\text{C}$ .

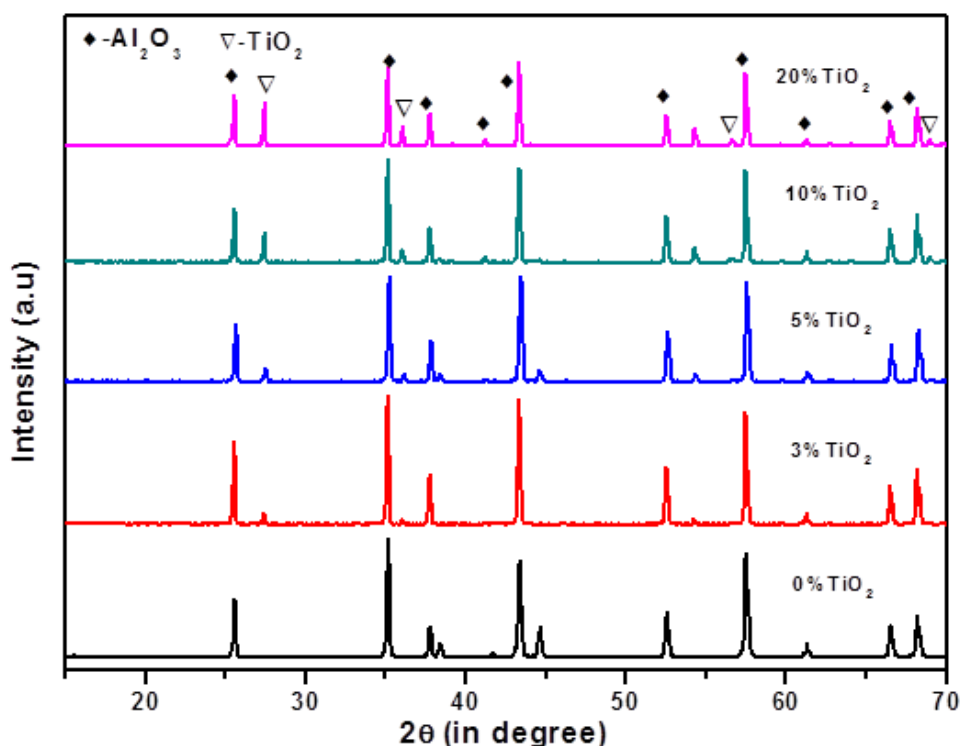
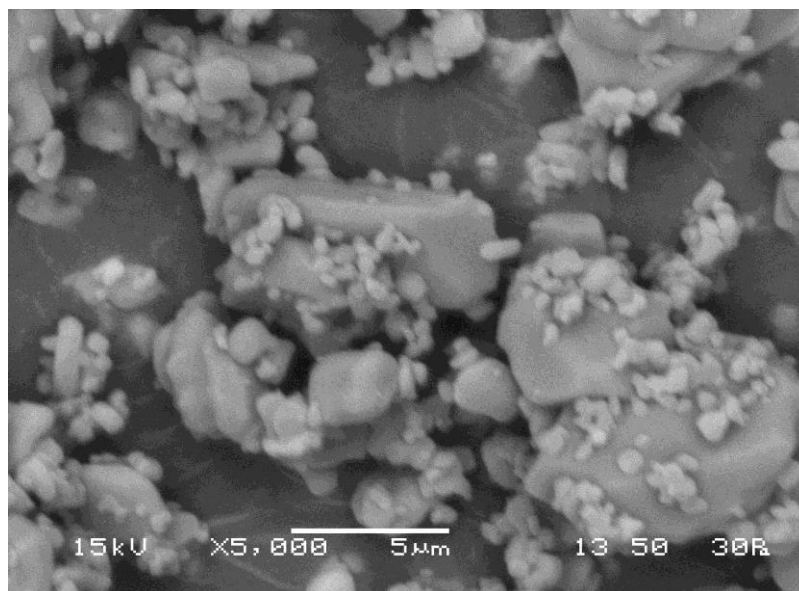


**Figure 7:** XRD plot of powder of different composition, calcined at  $1200^\circ\text{C}$

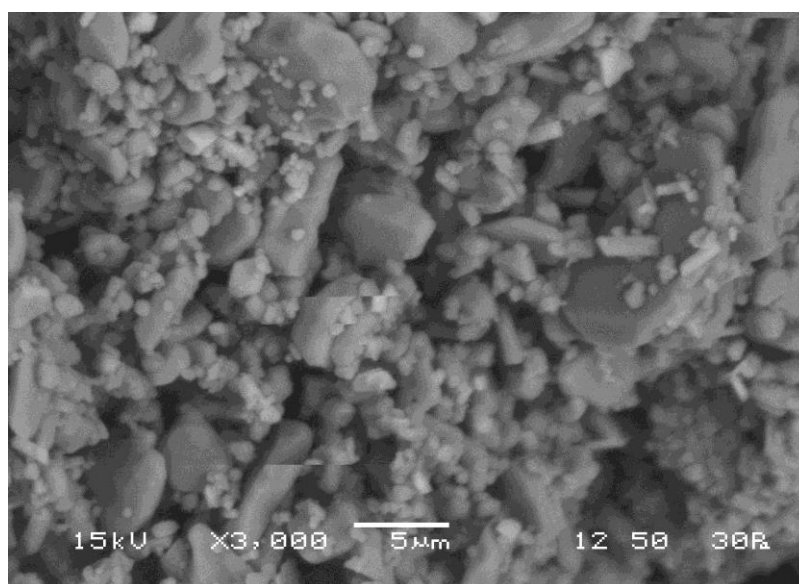
## 5.2 Morphology of calcined powders

The powder morphology of calcined powder for four compositions (3, 13, 20, 40 wt%  $\text{TiO}_2$ ) in Back Scattered Electron (BSE) mode is shown in Fig8. The bigger particles are  $\text{Al}_2\text{O}_3$  and the smaller particles are  $\text{TiO}_2$ . Alumina particle has size in the range of  $2\text{--}5\text{ }\mu\text{m}$  and  $\text{TiO}_2$  has size in the submicron range. With increase in  $\text{TiO}_2$  content more plate like

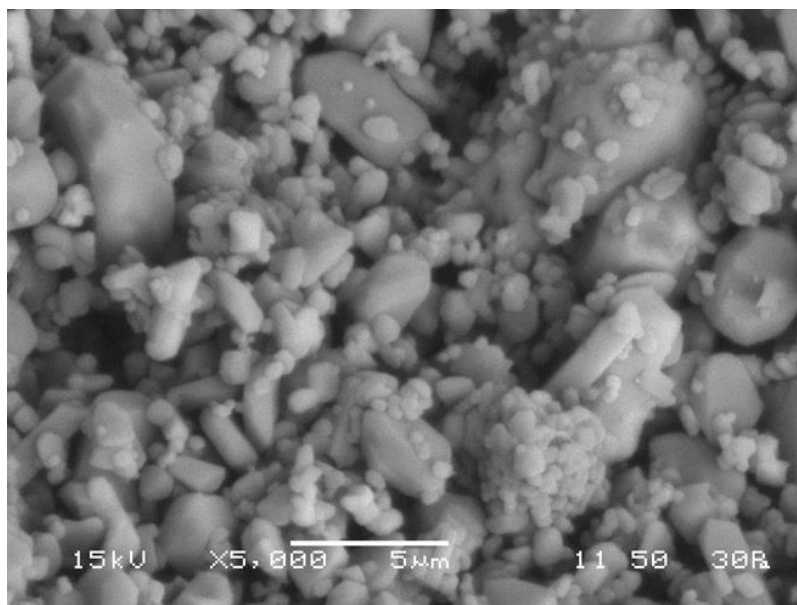
particles are visible in the structure. Composition having 40%  $\text{TiO}_2$  shows more plate like particles. It is unclear that  $\text{TiO}_2$  has any role in formation plate like structure.



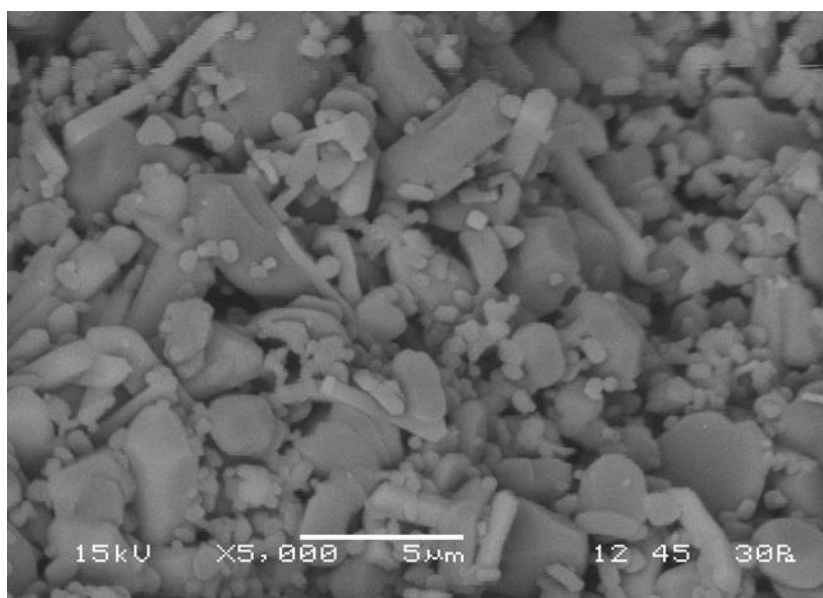
$\text{Al}_2\text{O}_3$ -3%  $\text{TiO}_2$



$\text{Al}_2\text{O}_3$ -13%  $\text{TiO}_2$



Al<sub>2</sub>O<sub>3</sub>-20% TiO<sub>2</sub>



Al<sub>2</sub>O<sub>3</sub>-40% TiO<sub>2</sub>

**Figure 8:** SEM micrograph of (a) 3% (b) 13% (c) 20% and (d) 40% TiO<sub>2</sub>-added alumina powder calcined at 1200°C for 2hrs



### 5.3 Phase Analysis of sintered samples

Fig.9 shows the XRD pattern of  $\text{Al}_2\text{O}_3$ - $\text{TiO}_2$  compositions sintered at  $1600^\circ\text{C}$ . It is evident from the figure that as the  $\text{TiO}_2$  content in the composition is increasing the secondary phase  $\text{Al}_2\text{TiO}_5$  (AT) is also increasing. For smaller percentage of  $\text{TiO}_2$ , a very small peak of AT phase was observed. It was seen that for high percentage (20 and 40 wt%  $\text{TiO}_2$ ) of  $\text{TiO}_2$  composition there is only  $\text{Al}_2\text{O}_3$  and AT phase is present.  $\text{TiO}_2$  phase is completely disappears for this compositions. That means,  $\text{TiO}_2$  is completely reacting with  $\text{Al}_2\text{O}_3$  and forming a secondary phase AT and it is stable at room temperature.

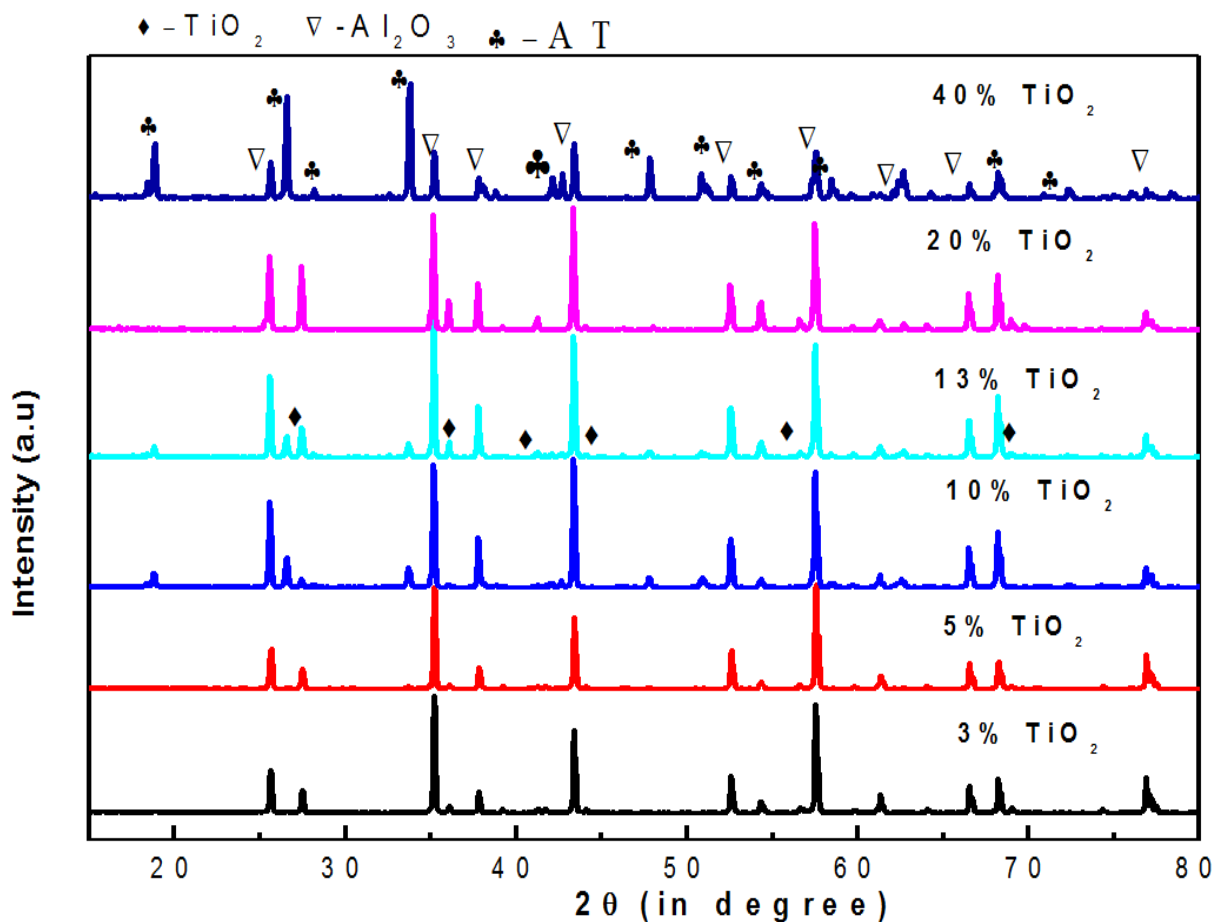


**Figure 9:** XRD pattern for sintered samples.

## 5.4 Densification behavior

Density of all the composition sintered at 1600°C was measured and it was observed that density (Fig.10) is increasing with increasing the percentage of TiO<sub>2</sub> in the composition for (3-5 % TiO<sub>2</sub>) then it is decreasing with higher amount of TiO<sub>2</sub>. Initial increase in density can be attributed to grain boundary modification and higher diffusion rate of ionic species. It is to be noted that pure alumina can be sintered to only less than 90% relative density at 1600°C. Lee et al. [8] got 99% of relative density by hot pressing for 5% TiO<sub>2</sub> added sample. We got more than 98% of density by pressureless sintering. The decrease in density for high amount of TiO<sub>2</sub> may be due to the formation of secondary AT phase which has lower density than alumina and titania. High temperature sintering (1650°C) of higher TiO<sub>2</sub> added sample failed to enhance the density. It is difficult to sinter Al<sub>2</sub>TiO<sub>5</sub> phase. Table 2 shows the bulk and relative density of different composition. Maximum density is achieved for 5% TiO<sub>2</sub> in alumina.

**Table 2:** Bulk density, Relative density and percent of different phases present in 6 different compositions sintered at 1600°C

Composition	Density (gm/cc) (1600°C)	Relative density	% of phase present Al <sub>2</sub> O <sub>3</sub> - Al <sub>2</sub> TiO <sub>5</sub> -TiO <sub>2</sub>
AT-3	3.806	96.15	97-0-3
AT-5	3.945	98.75	89-4-7
AT-10	3.97	97.96	86-13-2
AT-13	3.589	91.09	85-9-6
AT-20	3.383	87.36	69-31-0
AT-40	2.921	75.94	60-40-0

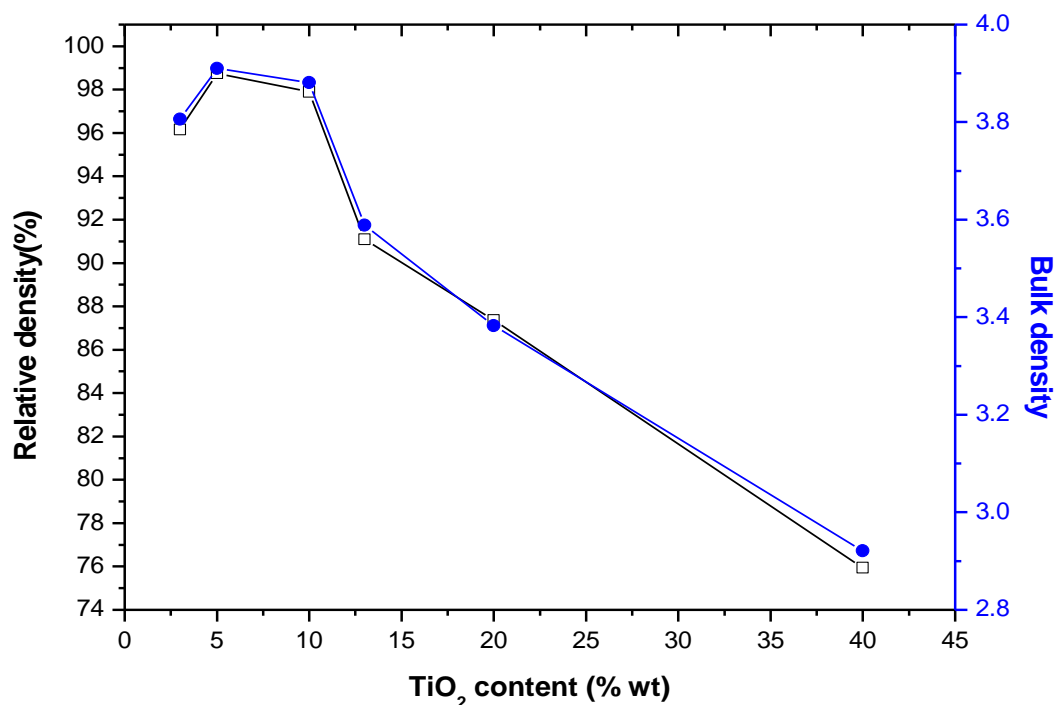
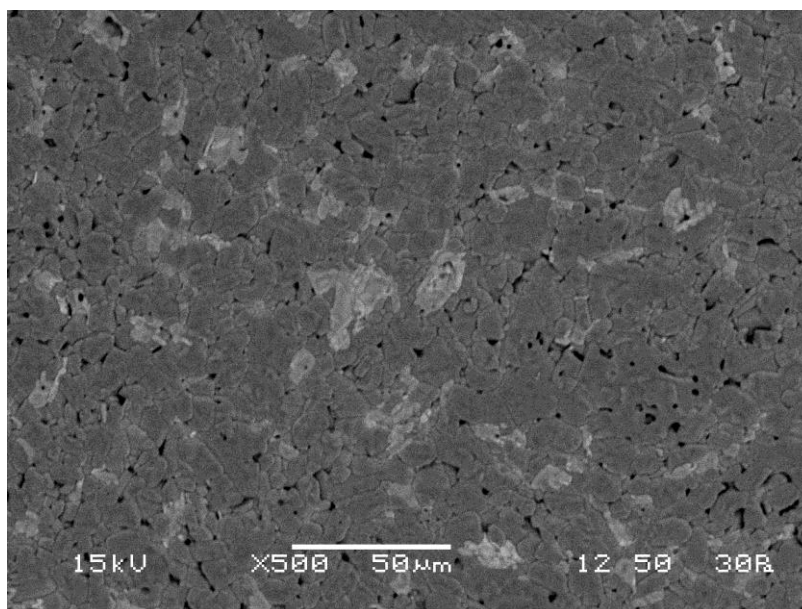


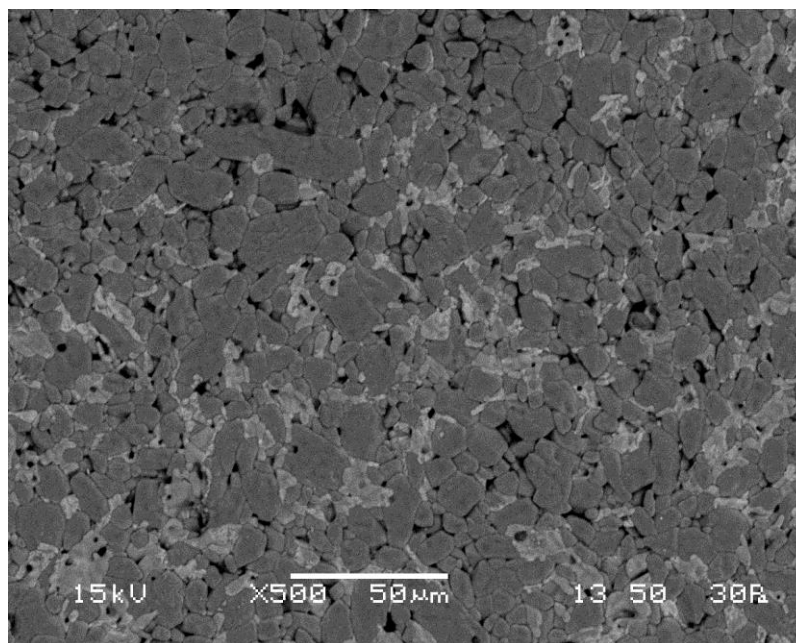
**Figure 10:** Plot for variation of relative density and bulk density with TiO<sub>2</sub> content.

### 5.5 Microstructure of sintered samples

The microstructure of sintered pellets (3 and 13 wt% TiO<sub>2</sub>) in Back Scattered Electron (BSE) mode is shown in Fig. 11. The dark grains are Al<sub>2</sub>O<sub>3</sub> and the bright grains are TiO<sub>2</sub>. It was observed that there is a nonuniform distribution grains of TiO<sub>2</sub> and Al<sub>2</sub>O<sub>3</sub> throughout the matrix. A slight increase in grain growth was observed in 13% TiO<sub>2</sub>-doped alumina compare to alumina having 3% TiO<sub>2</sub>. Small amount of large equiaxed grains are observed in AT1-13 sample. The average grain size of 13-15 μm was in AT-13 sample.



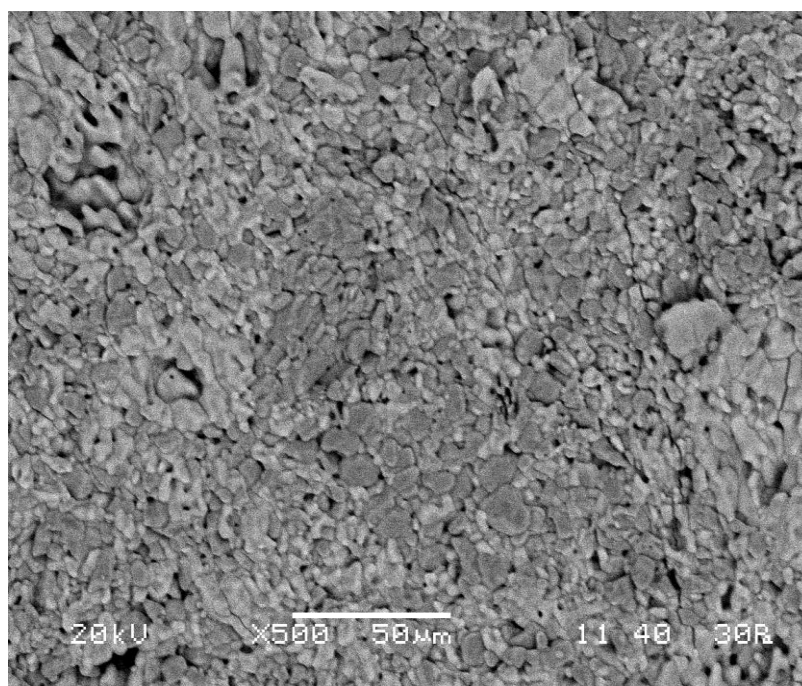
AT-3 ( $\text{Al}_2\text{O}_3$ -3%  $\text{TiO}_2$ )



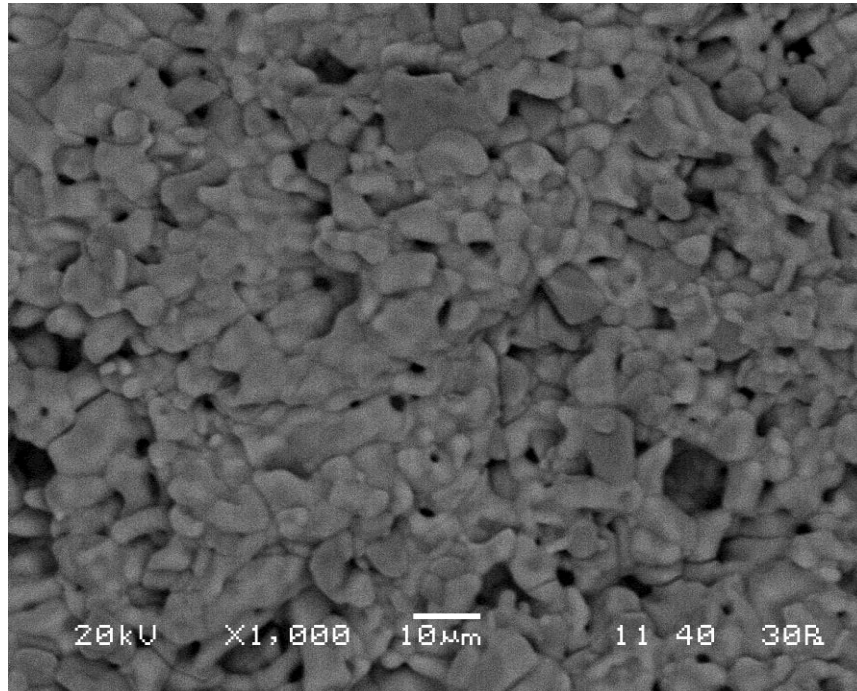
AT-13 ( $\text{Al}_2\text{O}_3$ -13%  $\text{TiO}_2$ )

**Figure11:** SEM micrograph of AT-3 and AT-13 sample sintered at 1600°C for 2hrs

Figure 12 shows the SEM micrograph of AT-20 and AT-40 sample. There is no clear phase of  $\text{TiO}_2$  is observed. As per the XRD pattern for sintered sample,  $\text{TiO}_2$  is completely reacting with alumina and forming secondary phase. Large numbers of pores is observed with increasing the  $\text{TiO}_2$  percentage. Secondary phase AT have lower density than alumina and  $\text{TiO}_2$ , decreases the density of the sample. In AT-20 sample two different contrast region observed in the microstructure. Details EDAX study required to find out the distribution of phases. For AT-40 sample this type of microstructure is absent.



$\text{Al}_2\text{O}_3$ -20%  $\text{TiO}_2$



$\text{Al}_2\text{O}_3$ -40%  $\text{TiO}_2$

**Figure 12:** SEM micrograph of AT-20 and AT-40 sample sintered at  $1600^\circ\text{C}$  for 2hrs.

## **5.6 Mechanical properties**

### **5.6.1 Flexural strength**

Flexural strength value gives material's ability to resist deformation under load. For measuring flexural strength, three-point bending was used. The value obtained is written in the table for different composition. Flexural strength is highest for 3%  $\text{TiO}_2$  in alumina (164 MPa) and it decreases with increase in the  $\text{TiO}_2$  content. Reduction in strength can be attributed to large size grain and equiaxed grain. This is to be mentioned that strength values of AT-20 and AT-40 should not be compared with other sample as those sample has very high density. The size effect and the thermal stress due to the difference of thermal expansion coefficients between  $\text{Al}_2\text{O}_3$  and  $\text{Al}_2\text{TiO}_5$  were considered to be the major factors for the reduction of the bending strength [16].

**Table 3:** flexural strength (in MPa) of sintered sample for different percentage of  $\text{TiO}_2$  in alumina.

TiO <sub>2</sub> content in Alumina(% wt)	Flexural strength (MPa)
3	155
5	42.9
10	17.23
13	23.53
20	22.25
40	14.458

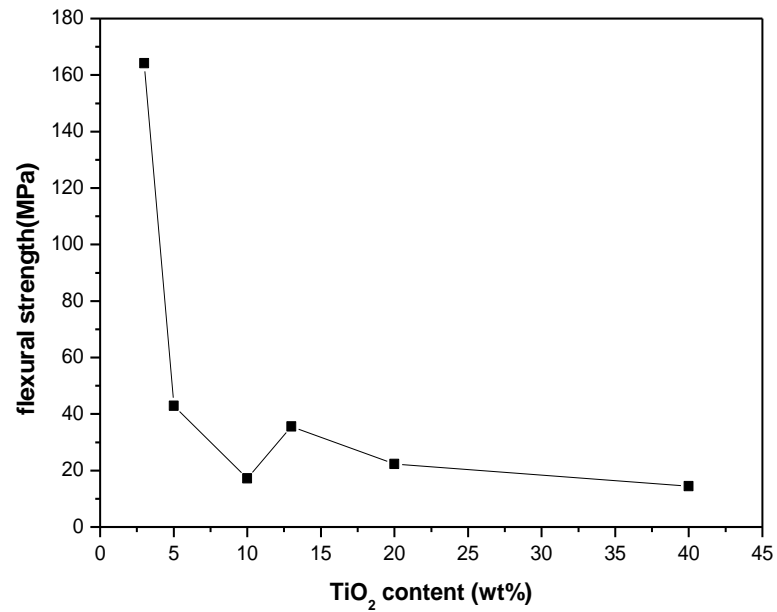


**Figure 13:** Flexural strength of different  $\text{TiO}_2$  added sample sintered at 1600°C

### 5.6.2 Vickers Hardness

Table 4 shows the value of hardness in GPa with respect to their composition. Highest value of hardness is achieved for 3%  $\text{TiO}_2$ , 15.658 GPa. With increasing the  $\text{TiO}_2$  content in the alumina hardness is decreasing but it was also seen that, increasing the percentage of  $\text{TiO}_2$  from 5 to 10. This increase of hardness is supposed that these increments are due to the presence of rutile and aluminum titanate phases disperse in alumina matrix. It is known that small quantities of  $\text{TiO}_2$  acts as a sintering aid and that dispersion of secondary phase increases and enhances mechanical properties.

This is to be mentioned that hardness values of AT-20 and AT-40 should not be compared with other sample as those samples have very high density. Alumina containing higher amount of  $\text{TiO}_2$  shows a rapid decrease in hardness. This decrease in hardness value may be due to the presence of high  $\text{Al}_2\text{TiO}_5$  phase which produces micro cracks instability of this phase.  $\text{Al}_2\text{TiO}_5$  decomposes and produces micro cracks at room temperature results in rapid decrease in hardness [11].

**Table 4:** hardness value in GPa for different percentage of  $\text{TiO}_2$  in alumina

<b><math>\text{TiO}_2</math> content (% wt)</b>	<b>Hardness (GPa)</b>
<b>3</b>	<b>15.658</b>
<b>5</b>	<b>13.034</b>
<b>10</b>	<b>13.8</b>
<b>13</b>	<b>12.63</b>
<b>20</b>	<b>4.185</b>
<b>40</b>	<b>1.75</b>



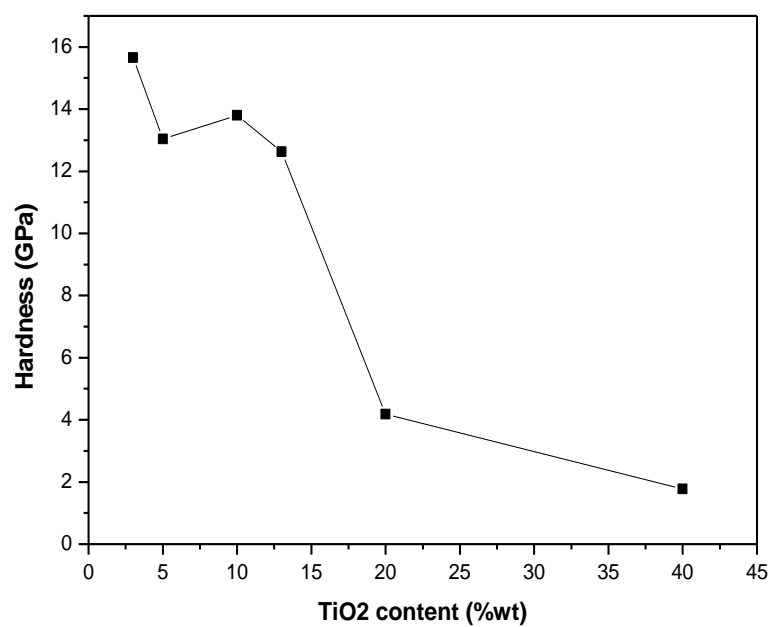


**Figure 14:** Vickers hardness of different TiO<sub>2</sub> added sample sintered at 1600°C.

## **Chapter 6**

# **CONCLUSIONS**

## Conclusions

The effect of  $\text{TiO}_2$  addition in alumina on phase formation, densification, microstructure and mechanical properties of the composite was studied. The ceramic composite were prepared with  $\text{Al}_2\text{O}_3$  and  $\text{TiO}_2$  powder by solid state mixing route. The  $\text{Al}_2\text{O}_3$ – $\text{TiO}_2$  powders contain 3, 5, 10, 13, 20, and 40 wt. % of  $\text{TiO}_2$ .

- Calcined powder contains only alumina and titania phase. No intermediate phase was detected because of alumina and titania starts reaction above  $1300^\circ\text{C}$ .
- In sintered sample  $\text{Al}_2\text{TiO}_5$  phase was detected and its concentration increases with increases in  $\text{TiO}_2$  content.  $\text{TiO}_2$  phase was disappeared for high amount of  $\text{TiO}_2$  (20 and 40wt% addition) addition.
- $\text{Al}_2\text{O}_3$  /  $\text{TiO}_2$  composite powder was sintered at  $1600^\circ\text{C}$  and giving maximum density for 5% $\text{TiO}_2$  addition. 98% of relative density was achieved by pressureless sintering. There is an increase of density is seen for 3-5 % $\text{TiO}_2$  and then density is decreasing rapidly with increase in  $\text{TiO}_2$  content. Initial increase in density may be attributed to grain boundary modification and higher diffusion rate of ionic species. The decrease in density for high amount of  $\text{TiO}_2$  may be due to the formation of secondary  $\text{Al}_2\text{TiO}_5$  phase which has lower density than alumina and titania and which is difficult to sinter.
- Flexural strength and Vickers hardness of  $\text{Al}_2\text{O}_3$ - $\text{TiO}_2$ - $\text{Al}_2\text{TiO}_5$  composite is dependent on the content of  $\text{TiO}_2$  and the presence of  $\text{Al}_2\text{TiO}_5$  phase. AT-3 and AT-5 shows very high hardness of 15.6 and 13.03 GPa respectively. Highest flexural strength (164.2 MPa) was observed for AT-3.

## References

1. Wan et al., Preparation of Nanocomposites of Alumina and Titania, US Patent 7,217,386 B2, May 15, 2007.
2. Hori, Tough Corundum-Rutile Composite Sintered Body, US Patent 4,892,850, Jan. 9, 1990.
3. Y.M. Wang, H. Tiana, X.E. Shen, L. Wena, J.H. Ouyang, Y. Zhou, D.C. Jia, L.X. Guo, "An elevated temperature infrared emissivity ceramic coating formed on 2024 aluminium alloy by microarc oxidation" *Ceramics International*, In Press.
4. Miriam Floristán, Philipp Müller, Andreas Gebhardt, Andreas Killinger, Rainer Gadow, Antonio Cardella, Chuanfei Li, Reinhold Stadler, Günter Zangl, Matthias Hirsch, Heinrich P. Laqua, Walter Kasperek, "Development and testing of 140GHz absorber coatings for the water baffle of W7-X cryopumps", *Fusion Engineering and Design* 86 (2011) 1847–1850,.
5. B.V. Cockeram, D.P. Measures, A.J. Mueller, "The development and testing of emissivity enhancement coatings for thermo photovoltaic (TPV) radiator applications" *Thin Solid Films* 355-356(1999), 17-25
6. <http://www.chemicals-technology.com>
7. *Ceramics Science and Technology* Riedel, R., & Chen, I. W. (2000).
8. Soo Whon Lee, Carlos Morillo S.W. Lee et al. "Tribological and microstructural analysis of Al<sub>2</sub>O<sub>3</sub>/TiO<sub>2</sub> nanocomposites to use in the femoral head of hip replacement"; *Wear* 255 (2003) 1040–1044.
9. R. Yılma, A.O. Kurt "Effects of TiO<sub>2</sub> on the mechanical properties of the Al<sub>2</sub>O<sub>3</sub>–TiO<sub>2</sub> plasma sprayed coating", *Journal of the European Ceramic Society* 27 1319–132(2007).
10. J.J. Meleán-Martínez, M. Jiménez-Melendo "High temperature mechanical behavior of aluminium titanate+mullite composites"; *Journal of the European Ceramic Society* 21, 63-70 (2001).
11. <http://www.webelements.com>
12. Jae Hyun Park, Won Jae Lee, and IlSoo Kim "Al<sub>2</sub>TiO<sub>5</sub>-machinable Ceramics Made by Reactive Sintering of Al<sub>2</sub>O<sub>3</sub> and TiO<sub>2</sub>", *Journal of the Korean Ceramic Society* Vol. 47, 498-502, (2010).

13. Hamanok, "Effect of TiO<sub>2</sub> on sintering of alumina ceramic", J. ceram. Soc. JAP. Vol. 94, 505 (1986).
14. G.Tiloca,"Thermal stabilization of aluminium-titanate and properties of aluminium-titanate solid solutions"; Journal of material science 26 2809- 2814(1991).
15. SerkanAball "Effect of TiO<sub>2</sub> doping on microstructural properties of Al<sub>2</sub>O<sub>3</sub>-based single crystal Ceramics" Journal of Ceramic Processing Research. Vol. 12, No. 1, pp. 21~25 (2011).
16. Chih-JenWang, Chi-Yuen Huang,"Effect of TiO<sub>2</sub> addition on the sintering behavior, hardness and fracture toughness of an ultrafine alumina".Materials Science and Engineering A 492 306–310(2008).
17. Y.P. Fu, C.C. Chang, C.H. Lin, T.S. Chin, Ceram. Int. **30** 41(2004).